NANO LETTERS

2008
Vol. 8, No. 1
189−194

Monitoring Single-Molecule Reactivity on a Carbon Nanotube

Brett R. Goldsmith,[†] John G. Coroneus,[‡] Alexander A. Kane,[†] Gregory A. Weiss,[§,‡] and Philip G. Collins*,[†]

Departments of Physics and Astronomy, Molecular Biology and Biochemistry, and Chemistry, University of California, Irvine, California 92697-2025

Received September 18, 2007; Revised Manuscript Received November 26, 2007

ABSTRACT

Using point-functionalized carbon nanotube devices, we demonstrate continuous, multihour monitoring of a single carboxylate group interacting with its immediate environment. The conductance of the nanotube device directly transduces single-molecule attachments and detachments in the presence of the carboxylate-selective reagent 1-ethyl-3-(3-dimethylaminopropyl) carbodiimide hydrochloride (EDC). Because only one carboxylate is present in the device, it can be studied through hundreds of reactions, providing the statistical accuracy to directly determine a 12 s lifetime of the carboxy–EDC complex. An additional instability of the complex is transduced in real time and observed to have a median lifetime of 2 ms. By determining a turnover time in good agreement with bulk measurements and simultaneously illuminating additional dynamics, these results demonstrate this platform's potential for complementing optical methods in single-molecule research.

Compared to conventional microelectronics, prototype nanoelectronic devices based on nanowires, carbon nanotubes, and clusters generally have extraordinarily high surface to volume ratios. This fact greatly enhances the sensitivity of such devices to the chemistry taking place on their surfaces and drives ongoing interest in their application as ultrasensitive chemical and biological sensors. For example, by tailoring the surface chemistry of nanoscale conductors, amperometric sensors have been demonstrated for a wide range of analytes.[1,2] Furthermore, the range of sensitivity is believed to extend to the single-molecule limit since one-dimensional conductors can be disproportionately effected by single scattering sites.[3−6] Electronic sensors with single-molecule precision could complement the optical techniques currently used for single-molecule research and, combined with other emerging technologies like cantilever-based detection, expand the variety of tools for investigating complex chemical processes.

Single-molecule chemical detection has been previously demonstrated using silicon nanowire electronic devices.[7−10] For example, Patolsky et al. reported 10% conductance fluctuations as virus particles in solution individually interacted with an antibody-coated nanowire.[7] Similar changes, though not necessarily with single-molecule resolution, have been observed using coated single-walled carbon nanotubes (SWCNTs).[11,12] These coated nanoconductors must be operated in extremely low analyte concentrations in order to distinguish discrete, single-molecule events. Furthermore, statistical interpretation of the events is complicated by the large numbers of potential binding sites. For example, low reactant concentrations can severely slow target reactions or complicate multispecies studies. Multiple bound molecules or binding sites also complicate interpretation since simultaneous and overlapping reactions occur within the data. Such characteristics significantly reduce the applicability of such devices for assays of chemical behavior at equilibrium.

An alternate architecture demonstrated here is one that contains only a single chemically active site in the electronic circuit. With one transduction site, measurements can be uniquely ascribed to a single location, and single-molecule interactions can be observed even in high, synthetically relevant analyte concentrations. The sensing element described here consists of a single carboxylate introduced electrochemically into the sidewall of a SWCNT, as depicted in Figure 1a. Carboxylates provide a versatile handle for a broad range of chemical attachments via amide linkages,[13] and we have chosen to monitor the highly chemoselective activation of carboxylates by EDC, a reaction used widely in chemical biology and in the derivatization of bulk nanotube materials.[14]

The device is fabricated by starting with an electrically connected, pristine SWCNT and then applying a recently described point-functionalization technique.[15] This technique, in which conductance monitoring is used to observe and control electrochemical modifications, allows SWCNT devices to be chemically tailored to incorporate individual or multiple sidewall defects. Subsequent modification and

* To whom correspondence should be addressed. E-mail: collinsp@uci.edu.
† Department of Physics and Astronomy.
‡ Department of Molecular Biology and Biochemistry.
§ Department of Chemistry.

10.1021/nl0724079 CCC: $40.75
Published on Web 12/19/2007

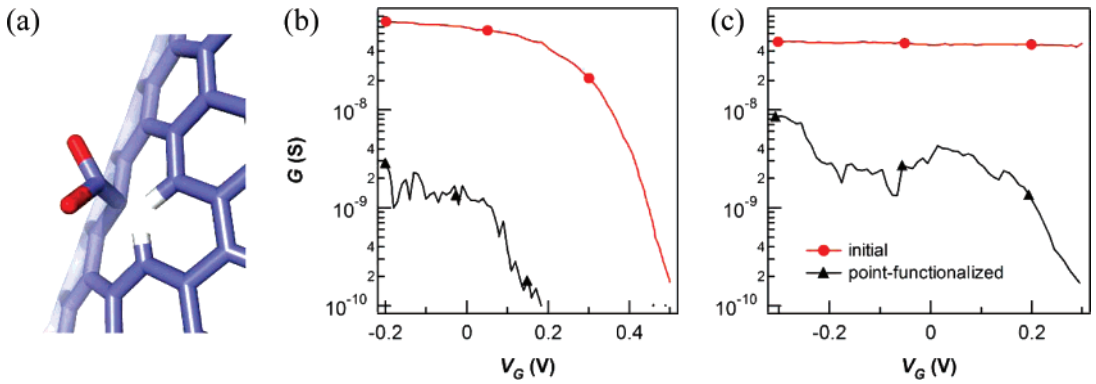

Figure 1. (a) Model for a carboxylate point defect electrochemically introduced into a SWCNT sidewall. (b,c) $G(V_g)$ characteristics for devices composed of one semiconducting SWCNT (b) and one metallic SWNCT (c). $G(V_g)$ is shown before (red) and after (black) point-functionalization of each device. The decrease in conductance and change in V_g sensitivity are attributed to the incorporation of a carboxylate.

differentiation of these defect sites provides a versatile starting point for single-site chemical sensing. For the data described here, devices were chosen in which a single SWCNT was connected to Pd electrodes. After initial electrical characterization in air, the Pd and SWCNT−Pd interfaces were passivated using PMMA, and each device was wire bonded and further encapsulated in insulating epoxy. Only 1 μm of the SWCNT sidewall, as exposed by e-beam lithography of the PMMA, was in direct contact with the liquid analytes when the device was submerged in solution.

Carboxylate functionalities were introduced by electrochemical acid oxidation (1 M H_2SO_4, $V_{SWCNT} = +0.9$ V vs Pt) combined with potassium permanganate exposure (6.5 mM $KMnO_4$).[15] To produce one carboxylate group on each SWCNT, the protocol featured application of $KMnO_4$ after a >99% drop in SWCNT conductance G.[16] All subsequent measurements were done in a conductive phosphate buffer[17] that can be used as a "liquid gate" to electrostatically modulate the SWCNT channel in three-terminal fashion.[18−20] Our gate voltage V_g is defined as the potential of the electrolyte, as measured with a Pt pseudoreference, with respect to the SWCNT source terminal. The device conductance was determined from the source−drain current measured under a constant DC bias of 100 mV.

Figure 1 shows typical characteristics of the conductance versus gate voltage $G(V_g)$ from SWCNT devices before and after introduction of carboxylates. Devices point-functionalized with carboxylates typically regain 1−10% of their initial conductivity and a strong gate dependence,[21] regardless of whether the initial SWCNT has a semiconducting band structure (Figure 1b) or a metallic band structure (Figure 1c). Scanning probe techniques indicate that the added resistance and gate sensitivity are concentrated and localized within the ∼50 nm resolution of these techniques, particularly when metallic SWCNTs are used.[3,4,15,22] Thus, though these quasi-ballistic systems cannot be accurately modeled as resistors in series, this localization has proven that the region immediately surrounding a carboxylate can be responsible for more than 90% of the two-terminal device resistance.[5,6,15,23]

The co-localization of the electrical resistance and the carboxylate functionalization provides the means for particularly sensitive electronic transduction of chemical events. Electric field sensitivity and enhanced scattering at the functionalized site can both play roles in converting chemical changes into conductance changes. To examine this hypothesis, we harness the single carboxylate as a catalyst in a simple reaction—the conversion of a reactive carbodiimide EDC into a mixed urea—and simultaneously monitor G and its fluctuations. Devices were monitored in phosphate buffer at pH 4.5 with and without the presence of 50 μM EDC.

Figure 2 shows representative portions from two several-hour measurements of a carboxylate-modified SWCNT. Figure 2a−c shows measurements taken without EDC. Conductance data are depicted at three time scale magnifications to illustrate the uniform fluctuation characteristics at all time scales. $G(t)$ wanders with a simple $1/f$ noise spectrum (Figure 2d) that provides a baseline for the device, regardless of the chemical environment. The $1/f$ spectra are very typical of SWCNT devices,[24,25] and we have confirmed that this remains generally true of our functionalized devices, whether measured in air or buffer.

The same device exhibits substantially different behavior when 50 μM EDC is present (Figure 2e−h). Pronounced $G(t)$ spikes and a broad noise spectrum appears. Inspection of $G(t)$ over short time segments clarifies that the additional features are due to an intermittent, rapidly oscillating, two-level fluctuator (Figure 2g). When active, this fluctuator increases the instantaneous $G(t)$ by as much as 50% through discrete jumps in conductance. Even though the fluctuator appears to have only two levels, its widely varying duty cycle leads to time-varying mean conductances, observed as spikes and plateaus in Figure 2e.

Approximately 10 point-functionalized devices have been prepared and tested in EDC. The appearance of a large-amplitude, high-speed fluctuator is common to all of the devices when measured with EDC, regardless of the initial SWCNT band structure. In each case, flushing EDC from the measurement cell reliably removes the fluctuator and restores the baseline noise spectrum of the device. As a further control, we have examined nonfunctionalized devices in EDC and observed typical $1/f$ spectra. We note that under special conditions of bias or temperature, large two-level fluctuators can add a Lorentzian peak to SWCNT[26−28] or

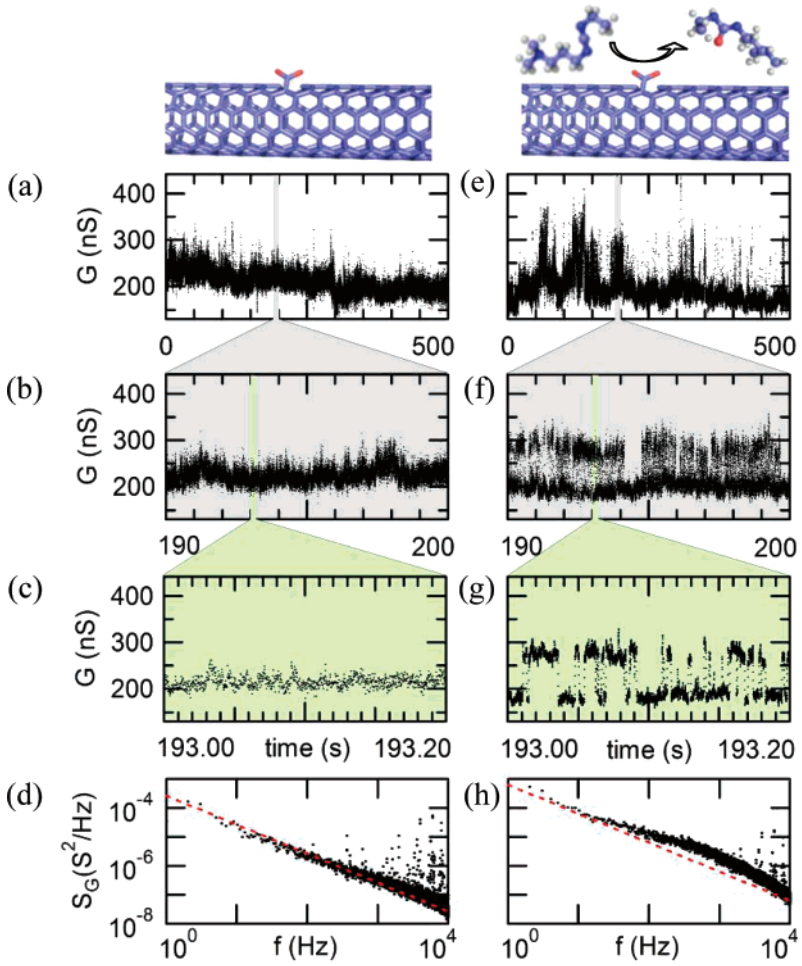

Figure 2. (a−c) $G(t)$ recordings of a carboxylate-functionalized SWCNT in phosphate buffer without EDC. The same data are depicted on 500, 10, and 0.2 s time axes (expanded about $t = 193$ s). (d) Averaged noise power spectrum S_G of the conductance data in (a). The dashed line (red) indicates the fit to $1/f$ behavior. (e−g) Measurements on the same device over similar time scales with 50 μM EDC added to the buffer, after 100 s have passed to allow for equilibration. Enhanced two-level switching is clearly visible at higher magnifications (f, g) and has variable duration during the experiment. (h) Averaged noise power spectrum corresponding to data in (e).

other nanodevice[29,30] spectra; in this paper, point-functionalized devices with anomalous noise spectra at any bias, in either air or buffer, have not been used for further measurements.

While it is tempting to directly attribute the differences observed in Figure 2 to reactions between the carboxylate and EDC, two experimental details quickly rule out a simple interpretation. First, the mean lifetime of the fluctuator resolved in Figure 2g is a mere 10 ms, whereas the EDC turnover time in bulk solutions can exceed 100 s.[31] Second, the fluctuator randomly starts and stops, even in the presence of excess EDC. For example, the fluctuator may be inactive for less than a second, as observed in the middle of Figure 2f, or for a few minutes, as demonstrated in Figure 2e, before becoming active again.

Thus, characterization of the $G(t)$ dynamics in the presence of EDC requires statistical analysis of conductance stability over multiple time scales. The high-speed jumps within each active period can be analyzed in terms of the time spent in high-current (τ_{hi}) and low-current (τ_{lo}) states. Simultaneously, a slower process causes the fluctuator to become active or inactive on the scale of tens to thousands of two-level fluctuations. Fortunately, it is straightforward to inspect $G(t)$ and enumerate the durations of each active (τ_{active}) and inactive ($\tau_{inactive}$) period. In the following analysis, each time period is considered separately, beginning with τ_{active}.

Approximately 60 distinct τ_{active} values are generated per hour of data acquisition. The complete data set (of which Figure 2e is a small subset) has a mean active duration of $<\tau_{active}> = 12.4 \pm 2.1$ s. Histograms of τ_{active} values can be fit to a normal Poisson process, as shown in Figure 3. The quality of this fit indicates that τ_{active} can be interpreted as a simple probability distribution; once activated, the probability that the fluctuation continues at time t follows the normal distribution $P(t) = (e^{-t/<\tau_{active}>})/<\tau_{active}>$, though a significant deviation occurs for long-lived events having $<\tau_{active}> >$ 40 s, which is examined below. A similar analysis of the corresponding inactive periods $\tau_{inactive}$ yields a mean duration of $<\tau_{inactive}> = 46.5 \pm 16.2$ s. The sum of $<\tau_{active}> + <\tau_{inactive}> = 58.9$ s constitutes an average cycle time for the fluctuator to go from one active period to another.

In bulk solutions, carboxylates provide nucleophilic, catalytic sites to which EDC binds and forms a transient and reactive intermediate species (termed an *O*-acylisourea).

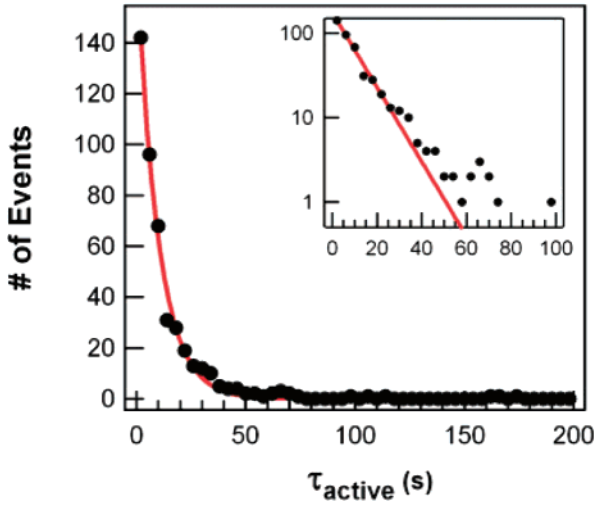

Figure 3. Histogram of τ_{active} values, plotted on linear and semilogarithmic (inset) axes. The red lines are a fit to a simple normal process with $<\tau_{active}> = 12.4$ s.

Hydrolysis liberates a mixed urea, freeing the carboxylate to bind another EDC molecule. This reaction can be characterized by a mean turnover time, a substantial fraction of which is determined by the stability of the acylisourea. Using reaction monitoring by UV absorbance, the bulk half-life of the EDC reaction near our experimental conditions has been measured as 100 s.[31] This value corresponds to a single-molecule turnover time of approximately 140 s.[31]

This turnover time, inferred from bulk measurements, is in reasonable agreement with the cycling of fluctuator activity described above. The faster turnover in the SWCNT experiment may be due to an exceptionally low concentration of carboxylate and a large excess of EDC, which should result in maximum reaction rate conditions. Since the active periods described above are only observed in the presence of EDC, we hypothesize that τ_{active} is associated with an EDC molecule being bound to the SWCNT carboxylate and that no EDC is bound when the two-level fluctuator is inactive. According to this interpretation, $<\tau_{active}>$ is a quantitative probability for the *O*-acylisourea intermediate to become hydrolyzed and released as urea. The $\tau_{inactive}$ parameter describes the time required before EDC capture. Though UV absorbance measurement of the turnover rate is comparatively easy, such bulk measurements do not allow the observation of intermediates. The SWCNT measurement, on the other hand, determines the intermediate lifetimes by monitoring single-molecule turnover events.

The value of $<\tau_{inactive}>$ is consistent with the experimental conditions used. Reaction with the carboxylate is considerably faster with biprotonated EDC, with the second protonation step having a pK_a of 3.5. Our experiments are run at pH 4.5, as part of a protocol optimized for protein coupling using the dual reagents EDC and NHS.[13] The resulting EDC deprotonation (approximately 90% at this pH), and perhaps noncovalent electrostatic interactions between carboxylate and EDC, can lengthen $<\tau_{inactive}>$ and slow the reaction rate.[32] This pH dependence provides an independent control of the reaction time to slow the on rate without requiring

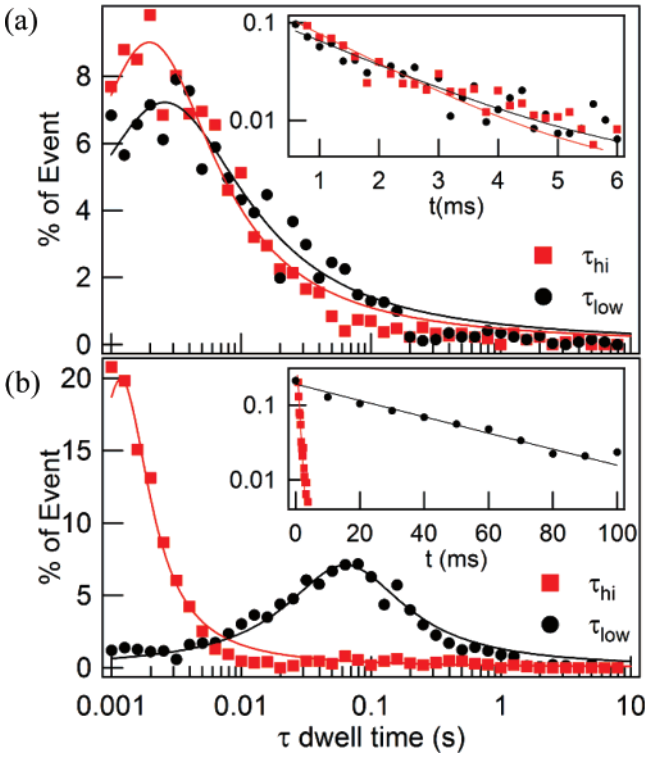

Figure 4. Histograms of τ_{hi} (red) and τ_{lo} (black) values, including a normalized probability distribution on semilogarithmic axes (inset). Solid lines are curve fits to the data, as described in the text. (a) A typical, symmetric two-level system having $<\tau_{hi}> = 2$ ms and $<\tau_{lo}> = 2$ ms. (b) An asymmetric active period having $<\tau_{hi}> = 1$ ms and $<\tau_{lo}> = 90$ ms. These two examples are separated in time by one inactive period.

operation in the diffusion-limited regime of previous single-molecule work.[7,9,10] Further investigation may allow the pH dependence of both time components to be mapped, though similar analysis will be difficult for very short $\tau_{inactive}$ intervals where the active fluctuation periods merge.

The assignment of τ_{active} as a chemically relevant half-life for a reactive intermediate affects the calculation and interpretation of the mean times $<\tau_{hi}>$ and $<\tau_{lo}>$. For example, $<\tau_{lo}> = 13$ ms in Figure 2g, yet the fluctuator remained in its low-current state for nearly 20 s shortly before becoming active. Determining meaningful values of $<\tau_{hi}>$ and $<\tau_{lo}>$ therefore requires that long periods corresponding to $\tau_{inactive}$ be explicitly excluded from the averaging of τ_{hi} and τ_{lo}. The separation of data into active and inactive periods, as described above, aids this processing and further allows a comparison of $<\tau_{hi}>$ and $<\tau_{lo}>$ values from one active period to another.

Figure 4a depicts representative histograms of τ_{hi} and τ_{lo} events observed during a single active fluctuation period. These histograms can be used to calculate the probability distribution functions for τ_{hi} and τ_{lo}, which in turn fit simple exponential decays characteristic of Poisson processes. The inset to Figure 4a shows the measured distribution and its fit on semilogarithmic axes. The main figure shows the same distribution multiplied by the dwell time, equivalent to the percentage of time spent at a particular τ_{hi} or τ_{lo}, with peaks corresponding to $<\tau_{hi}>$ and $<\tau_{lo}>$. In approximately 90% of the active periods analyzed, τ_{hi} and τ_{lo} have nearly equal

distributions and means, and the distributions suggest an individual fluctuator rather than a collection of two-level systems.

Similar analysis of the τ_{hi} and τ_{lo} probability distributions from each active period proves that these distributions and their mean transition rates vary from one active period to the next. A cumulative histogram of τ_{hi} and τ_{lo} values from several active periods cannot be assigned to only a single peak. Furthermore, in approximately 10% of the active periods, highly asymmetric distributions are observed, where either the high or the low conductance state is strongly preferred (Figure 4b). Within the resolution of the data sets, the changes in the probability distributions seem to occur in an abrupt, step-like manner during the inactive periods. This variation demands that the fluctuators of different active periods be analyzed separately; it further requires a simple way of characterizing fluctuators for comparison.

The study of two-level fluctuations in electronic devices is a well-developed field, particularly for silicon devices in which localized trap states interact with conduction channels.[29] Typically, the dynamics of these systems are bias- and temperature-dependent, reflecting a slight energy difference ΔE between the two stable conductance states.[29] From measured τ_{hi} and τ_{lo} values, this energy difference may be calculated as $\Delta E = k_B T \ln(<\tau_{lo}>/<\tau_{hi}>)$. Such standard analysis offers a useful tool for determining causes of two-level noise in silicon electronics.[29]

The conductance fluctuations transduced from the *O*-acylisourea complex provide an analogous two-state process. In this case, the highly resistive, point-functionalized site on the SWCNT sidewall is sensitive to charge−charge and dipole−dipole interactions with surrounding molecules. The attached acylisourea may strongly interact with the SWCNT conductance due to its attachment to the point-functionalized site. This interaction could be as simple as providing a trap state near the nanotube, analogous to the silicon oxide traps which cause two-level fluctuations in silicon transistors. However, many possible interactions between the acylisourea and the nanotube, the surrounding liquid environment, or the point-functionalized site could lead to the observed two-level switching. Without presuming to solve for the responsible degree of freedom in the acylisourea or its attachment, we can assume a generic model of two states separated by ΔE to further examine the fluctuation dynamics.

Figure 5 plots the values of ΔE calculated for each of the active periods described above. Symmetric fluctuations with small $|\Delta E|$ are most prevalent in the data and account for over 75% of the active periods. This main cluster of data is visible as the central peak in Figure 5. However, the distribution has one other statistically significant population with substantially different behaviors. Approximately 11% of the active periods are highly asymmetric, with $\Delta E < -7\ k_B T$.[33] When the mean lifetime $<\tau_{active}>$ is calculated separately at each ΔE, these asymmetric fluctuators are observed to form a cluster with unusually long lifetimes (Figure 5). As a subgroup, this cluster is responsible for the long tail in the τ_{active} distribution plotted in Figure 3, as well as the deviation of the data from the curve fit at $\tau > 40$ s.

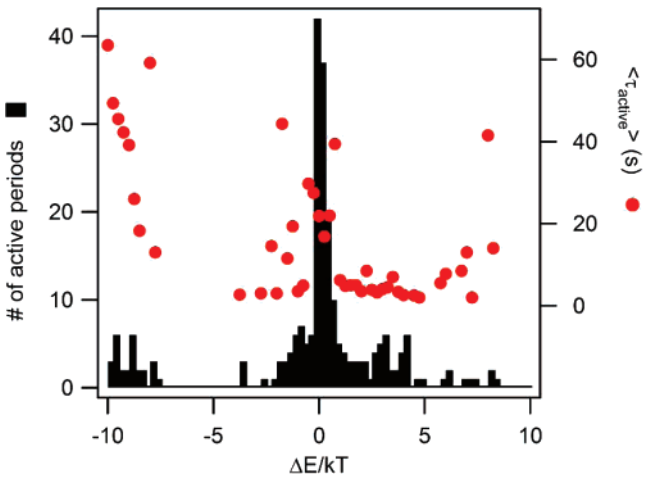

Figure 5. Histogram of ΔE values shows the preponderance of active events have symmetric fluctuators with $\Delta E \sim 0$ (black). Fluctuators with ΔE of a few $k_B T$ tend to have relatively short lifetimes (red), except for a population of unusually long-lived fluctuators with $\Delta E < -7\ k_B T$.

In addition, the average conductance change for the main group of active periods is 66 nS, while in the separated subgroup, the conductance change is much smaller at 22 nS. We note that the active events in this subgroup are not randomly distributed in time. Instead, they cluster together with most (19 of 27) occurring among 7 groups of asymmetric events.

These large $|\Delta E|$ events may be due to aging of the analyte solution or perhaps chemical variability of the attachment surface. For example, two broken carbon−carbon bonds sit immediately adjacent to the SWCNT carboxylate (Figure 1c), and the tautomerization or protonation of these may affect EDC binding. Alternately, EDC protonation, which should affect about 10% of the molecules at pH 4.5, could be responsible for substantially stronger interactions with the SWCNT than the *O*-acylisourea of the unprotonated EDC. Consistent with this hypothesis, the doubly protonated *O*-acylisourea could form stronger charge−charge or dipole interactions with the SWCNT, leading to its greater stability. Such stronger interactions would be expected to result in the long $<\tau_{active}>$ values and large $|\Delta E|$ values observed here.

In conclusion, point-functionalized SWCNT devices can provide a novel electronic platform for studying single-molecule chemical events. Electronic transduction by the SWCNT device conductance clearly illuminates the carboxylate reaction with EDC and the subsequent hydrolysis of the reactive intermediate. The technique can also provide an accurate ensemble measurement of kinetic rates in addition to direct observation of the lifetimes for intermediates. The single-molecule resolution of the technique further indicates some of the underlying chemical variability of the EDC−carboxylate interaction. The SWCNT device is sufficiently stable that measurements can be performed for long periods in diverse chemical environments, suggesting broad applicability for ongoing chemical and biochemical studies.

Acknowledgment. The authors gratefully acknowledge NSF support (EF-0404057) and helpful conversations with

Reginald Penner, Nancy Allbritton, and Doug Tobias. P.G.C. and B.R.G. acknowledge support from the NSF (DMR-0239842 and CHE-0533162) and a CalIT2 Emulux Fellowship.

References

(1) Katz, H. E. *Electroanalysis* **2004**, *16*, 1837.
(2) Yang-Kyu, C.; Xing-Jiu, H. *Sens. Actuator, B* **2007**, *122*, 659.
(3) Bockrath, M.; Liang, W. J.; Bozovic, D.; Hafner, J. H.; Lieber, C. M.; Tinkham, M.; Park, H. *Science* **2001**, *291*, 283.
(4) Freitag, M.; Johnson, A. T.; Kalinin, S. V.; Bonnell, D. A. *Phys. Rev. Lett.* **2002**, *89*, 216801.
(5) Park, H.; Zhao, J. J.; Lu, J. P. *Nanotechnology* **2005**, *16*, 635.
(6) Lee, Y.-S.; Marzari, N. *Phys. Rev. Lett.* **2006**, *97*, 116801.
(7) Patolsky, F.; Zheng, G.; Hayden, O.; Lakadamyali, M.; Zhuang, X.; Lieber, C. M. *Proc. Natl. Acad. Sci. U.S.A.* **2004**, *101*, 14017.
(8) Li, Z.; Rajendran, B.; Kamins, T. I.; Li, X.; Chen, Y.; Williams, R. S. *Appl. Phys. A* **2005**, *80*, 1257.
(9) Patolsky, F.; Timko, B. P.; Yu, G. H.; Fang, Y.; Greytak, A. B.; Zheng, G. F.; Lieber, C. M. *Science* **2006**, *313*, 1100.
(10) Fang, Y.; Patolsky, F.; Lieber, C. M. *Biophys. J.* **2007**, 551A.
(11) Star, A.; Gabriel, J. C. P.; Bradley, K.; Gruner, G. *Nano Lett.* **2003**, *3*, 459.
(12) Besteman, K.; Lee, J. O.; Wiertz, F. G. M.; Heering, H. A.; Dekker, C. *Nano Lett.* **2003**, *3*, 727.
(13) Grabarek, Z.; Gergely, J. *Anal. Biochem.* **1990**, *185*, 131.
(14) Banerjee, S.; Hemraj-Benny, T.; Wong, S. S. *Adv. Mater.* **2005**, *17*, 17.
(15) Goldsmith, B. R.; Coroneus, J. G.; Khalap, V. R.; Kane, A. A.; Weiss, G. A.; Collins, P. G. *Science* **2007**, *315*, 77.
(16) Coroneus, J. G.; Goldsmith, B. R.; Lamboy, J.; Kane, A. A.; Collins, P. G.; Weiss, G. A. In preparation.
(17) Phosphate buffer prepared using dibasic sodium phosphate (Fisher Scientific) and phosphoric acid (pH 4.5) diluted with DI water to 0.02 M.
(18) Kruger, M.; Buitelaar, M. R.; Nussbaumer, T.; Schonenberger, C.; Forro, L. *Appl. Phys. Lett.* **2001**, *78*, 1291.
(19) Rosenblatt, S.; Yaish, Y.; Park, J.; Gore, J.; Sazonova, V.; McEuen, P. L. *Nano Lett.* **2002**, *2*, 869.
(20) Mannik, J.; Goldsmith, B. R.; Kane, A.; Collins, P. G. *Phys. Rev. Lett.* **2006**, *97*, 16601.
(21) Overoxidized devices, which presumably contain multiple carboxylates, often recover less than 1% of their initial conductance.
(22) Fan, Y.; Goldsmith, B. R.; Collins, P. G. *Nat. Mater.* **2005**, *4*, 906.
(23) Bachtold, A.; Fuhrer, M. S.; Plyasunov, S.; Forero, M.; Anderson, E. H.; Zettl, A.; McEuen, P. L. *Phys. Rev. Lett.* **2000**, *84*, 6082.
(24) Collins, P. G.; Fuhrer, M. S.; Zettl, A. *Appl. Phys. Lett.* **2000**, *76*, 894.
(25) Snow, E. S.; Novak, J. P.; Lay, M. D.; Perkins, F. K. *Appl. Phys. Lett.* **2004**, *85*, 4172.
(26) Liu, F.; Bao, M. Q.; Kim, H. J.; Wang, K. L.; Li, C.; Liu, X. L.; Zhou, C. W. *Appl. Phys. Lett.* **2005**, *86*, 163102.
(27) Reza, S.; Huynh, Q. T.; Bosman, G.; Sippel-Oakley, J.; Rinzler, A. G. J. *Appl. Phys.* **2006**, *99*, 114309.
(28) Peng, H. B.; Hughes, M. E.; Golovchenko, J. A. *Appl. Phys. Lett.* **2006**, *89*, 243502.
(29) Kirton, M. J.; Uren, M. J. *Adv. Phys.* **1989**, *38*, 367.
(30) Mihaila, M. N. Low-frequency noise in nanomaterials and nanostructures. In *Noise and fluctuations control in electronic devices*; Balandin, A., Ed.; American Scientific: Valencia, CA, 2002.
(31) Wrobel, N.; Schinkinger, M.; Mirsky, V. M. *Anal. Biochem.* **2002**, *305*, 135.
(32) Xie, S. N. *Single Mol.* **2001**, *2*, 229.
(33) We do not expect, and have not observed, diffusion-limited processes using concentrations down to 10 μM.
(34) A substantial fraction of the 100 mV applied voltage bias is dissipated at the site of point-functionalization, providing many kT to the excitation of energetically deep two-level systems.

NL0724079